SPE-197457-MS

Deep Learning for a Fast and Accurate Prediction of Complex Carbonate Rock Permeability From 3D Micro-CT Images

Moussa Tembely, Khalifa University; Ali AlSumaiti, Abu Dhabi National Oil Company

This paper was prepared for presentation at the Abu Dhabi International Petroleum Exhibition & Conference held in Abu Dhabi, UAE, 11-14 November 2019.

Abstract

Correctly predicting subsurface flow properties is critical in many applications, ranging from water resource management to the petroleum industry. In the present paper, we establish a workflow to apply machine and deep learning (DL) to quickly and accurately compute petrophysical properties based on micro-CT images without any computationally intensive procedures. The pore network modeling (PNM) approach is widely used for fast computation of flow properties, albeit with less accuracy due to the inherent simplification of the pore space. Alternatively, direct simulation, such as the lattice Boltzmann method (LBM) is very accurate; however, its high computational cost prevents this approach from including all the relevant flow physics in a single simulation. After assessing numerical techniques ranging from PNM to the LBM, a framework based on machine learning (ML) is established for a fast and accurate prediction of permeability directly from 3D micro-CT images of complex Middle-East carbonate rock. We use thousands of samples from which engineered features—based on pore network modelling and images analysis—are fed into both shallow and deep learning algorithms to compute, as an output, the permeability in an end-to-end regression scheme. Within a supervised learning framework, algorithms based on linear regression, gradient boosting, support vector regression, and convolutional neural networks are applied to predict porous rock petrophysical properties from 3D micro-CT images. In addition, a hybrid neural network accounting for both the physical properties and 3D raw images is investigated. Finally, the estimated permeability of a complex carbonate by ML is found to be in good agreement with a more intensive simulation by voxel-based direct simulation. Furthermore, a significant gain in computational time—approximately three orders of magnitude—is achieved by applying ML compared to the LBM. This work highlights the critical role played by features engineering in predicting petrophysical properties using DL. The proposed workflow, combining deep learning and rock imaging and modeling, has great potential in reservoir simulation and characterization to swiftly and accurately predict petrophysical properties of porous media.

Introduction

Characterizing complex rocks, such as carbonate, is still very challenging due to intrinsic heterogeneities occurring at all scales of observation and measurement (Andrä et al., 2013a). The permeability—a function of the complex microstructure of the pore space—is one of the most significant petrophysical properties for

reservoir rock. It is essential in targeting a desired commercial oil and gas production rate (Kegang, 2012). Since there is no universal relationship for permeability, efficient tools to estimate it are desirable and are the subject of ongoing research (Chung, Wang, Armstrong, & Mostaghimi, 2019; Dehghan Khalili et al., 2013; Kegang, 2012; Singh, 2019).

One of the limitations of digital rock physics (DRP) is the computational power and resource required to perform accurate simulations. Petrophysical properties simulations at the pore scale can be classified into two categories: (i) pore-network modeling (Dong & Blunt, 2009) and (ii) direct modeling, which includes the finite difference method (Mostaghimi, Blunt, & Bijeljic, 2013), the finite element method (Andrä et al., 2013b), the finite volume method (Guibert et al., 2015; Tembely, AlSumaiti, Jouini, & Rahimov, 2017) and the lattice Boltzmann method (LBM) (Blunt et al., 2013). In place of direct simulation to predict the petrophysical properties, the pore network model (PNM) is preferred due to its simplicity. However, this approach, which is based on simplifying the geometry of the pore space, does not provide an accurate estimation. In order to circumvent the limitation inherent to the PNM model, we will develop a machine learning (ML) algorithm to achieve an accurate and fast numerical computation of the permeability. The developed framework can be extended to any multiphase flow properties of porous media.

Currently, ML is one of the most popular scientific research trends within artificial intelligence (AI) and has progressed rapidly in recent years, as the use of ML to analyze complex interactions has gained attention. ML has been applied to tackle many industrial applications ranging from engineering problems (Kohli & Arora, 2014; Nwachukwu, Jeong, Pyrcz, & Lake, 2018), to medical diagnostics (Yala, Lehman, Schuster, & Barzilay, 2019). Nevertheless, in petroleum engineering, most of the applications are concerned with reservoir characterization, petrophysical properties estimation from wells, rock typing, and production, as well as, very recently, drilling optimization (Pollock et al., 2018). Few works have been devoted to direct prediction of petrophysical properties using 3D micro-CT images. Although neural networks provide superior predictive capabilities in complex problems, little effort has been devoted to applying it to DRP for predicting petrophysical properties. However, recently, (Sudakov, Burnaev, & Koroteev, 2018) attempted to predict permeability using ML; however, the model depends on the less reliable PNM approach as an output of the ML algorithm. In addition, the analysis and incorporation of petrophysical features engineering were not considered. Finally, in (Wu, Yin, & Xiao, 2018), ML is used on simple 2D synthetic images without correlation with actual rocks for predicting the permeability.

Despite the widespread applications of PNM in DRP, the method exhibits some inherent limitations. One of the drawbacks of the PNM is that the model relies on a simplified pore-space to describe fluid flow through (more or less complex) porous media. In order to remediate these shortcomings, it is essential to directly solve flow governing equations on pore geometry without any simplification. However, due to the high computational cost of the LBM, it is challenging to account for all the relevant physical processes and details of the pore space (Xie, Raeini, Wang, Blunt, & Wang, 2016).

In most approaches, the premise is that the permeability derived from PNM represents the actual permeability of the sample. In fact, as we show in the present paper, there is a substantial discrepancy between the more accurate computation of the permeability using the LBM and the value from PNM. In that context, machine (deep or not) learning could be an attractive alternative for predicting petrophysical properties.

In the present paper, using 3D micro-CT images of complex carbonate rock from the Middle East, a comparative study of three numerical techniques used to simulate flow properties will be assessed in the context of DRP. A pore-network is generated from the segmented images using a maximal ball algorithm, and the simplified network is then used as an input of the PNM simulation for computing both the permeability and the electric formation factor. In addition, from the same segmented images, more complex geometry is constructed and meshed in order to perform the finite volume method (FVM) computation of the permeability. Finally, a voxel-based method of the LBM is employed to predict the permeability directly from the binary images. The computationally intensive nature of the simulations is highly related

to the complexity of the pore space generated, while the accuracy is affected by simplifying the pore space. Finally, a machine (deep or not) learning framework based on thousands of samples is detailed for a fast and accurate estimation of the permeability of 3D micro-CT images.

Fluid Flow Properties Computation

In order to estimate flow properties, we have combined ML and numerical techniques to simulate fluid flow behavior within a porous 3D digital rock (Figure 1). In this work, we will mainly focus on the estimation of the permeability, which can be regarded as a complex function of many variables, such as the porosity, the rock type, and the geometry of the pore space in addition to the pores' connection and distribution within the pore space. The framework developed will help to establish cost-effective and accurate modeling for permeability prediction of rocks.

Figure 1—Micro-CT image 500x500x920 voxels at 0.48 µm of a complex carbonate sample used for applying the machine and deep learning workflow.

The machine (deep or not) learning algorithm will be trained, tested, and validated on a dataset generated using two widely-used approaches: network modeling and direct simulation. This will be accomplished through 3 numerical techniques: pore network modeling (PNM), the finite volume method (FVM) and the lattice Boltzmann method (LBM). These techniques are detailed below.

Pore-network modelling

PNM simulation entails a network of pores and throats that topologically corresponds to the pore structure of the rock, which was extracted directly from the micro-CT images. The flow rates (Q_{ij}) within the throats of the network are given by:

$$Q_{ij} = -\frac{r_{ij}2}{8\mu l_{ij}}\left(p_j - p_i\right) \tag{1}$$

where p_i and p_j are the pressures at node i and j, l_{ij} is the pore throat length, and r_{ij} pore-throat radius, and µ is the viscosity. The quantitative predictive potential of PNM was investigated on pore-networks extracted using the maximal ball algorithm. Following the resolution of the continuity equation and using Darcy's law, the permeability can be expressed as follows:

$$K = \frac{\mu L Q_o}{A_o \Delta P}, \tag{2}$$

where L is the length of the sample, Q_o is the flow rate computed by integration from the outlet of the sample, and A_o corresponds to the outlet surface area, while ΔP corresponds to the pressure gradient. In addition

to the permeability, the formation resistivity factor was computed as well, which quantifies the impact of pore space on the electric resistance of the sample.

Finite volume method

The FVM is implemented to solve fluid flow equations within the porous media by discretizing the following mass and momentum conservation equations:

$$\nabla.\mathbf{V} = 0, \tag{3}$$

$$\rho\mathbf{V}\nabla\mathbf{V} = -\nabla p + \nabla.(\mu\nabla\mathbf{V}), \tag{4}$$

where **V** represents the velocity of the assumed-incompressible fluid of density ρ and viscosity μ.

The pore space was generated from the micro-CT image and meshed, details of which can be found in (Tembely et al., 2017). Subsequently, the permeability was calculated using the relation given in Eq. (2).

Lattice Boltzmann method

An LBM technique of a single-time relaxation scheme based on the Bhatnagar-Gross-Krook (BGK) collision operator was used to predict the permeability. A fluid consisting of fictive particles of distribution $f(x, t)$ satisfies the following evolution equation:

$$f\left(x + e_i, t + 1\right) = \frac{1}{\tau}\left(f(x, t) - f_{eq}(x, t)\right) \tag{5}$$

where τ is the relaxation time and e_i is the particle velocity in the i^{th} direction. Finally, based directly on the binary images, the permeability was derived similarly using Darcy's law (Eq. 4).

Regarding the application of the numerical techniques, we considered sub-samples extracted from the complex carbonate image provided in Figure 1. The dataset consisted of 1100 segmented samples of size 100x100x160 voxels at 0.48 μm resolution. In order to apply the PNM technique to the segmented images, we first extracted the network using the maximal ball algorithm (Dong & Blunt, 2009). Figure 2 depicts the statistics of the pore structure from 3 samples, where we provide the pore-network structure in terms of pore diameter, throat diameter, and length distribution, exhibiting complex pore spaces over a wide range of length scales.

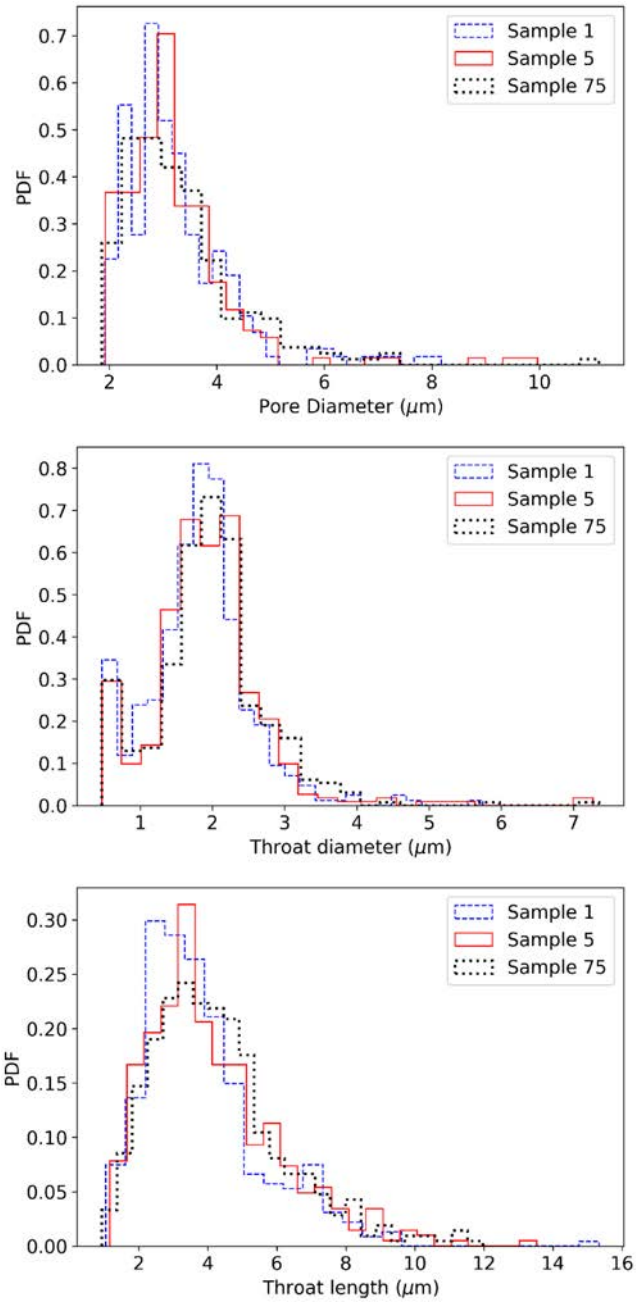

Figure 2—Statistics of carbonate and sandstone pore-network extraction.

To estimate flow properties, numerical simulations were performed using the three numerical techniques: PNM, FVM, and LBM. For illustration purposes, Figure 3 shows the schematic of the geometry required for the three techniques to simulate the permeability from a rock scanned at high resolution.

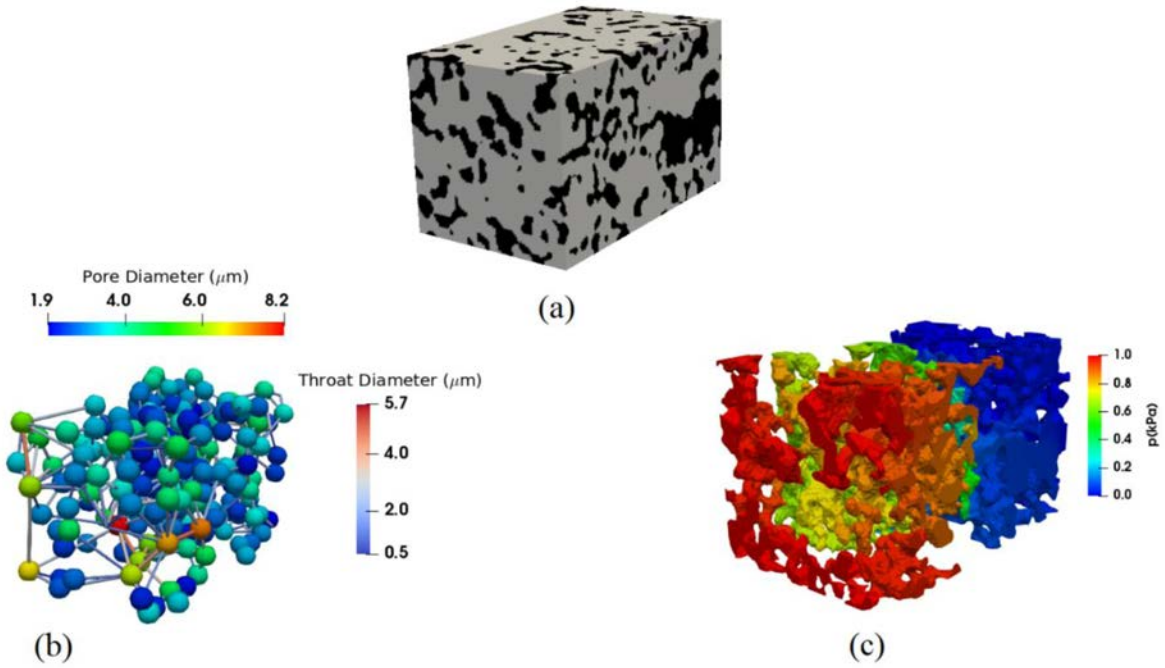

Figure 3—Approach and geometry used for (a) LBM, (b) PNM, and (c) FVM simulations of sample #1 scanned at high resolution.

We summarize the simulated values of the permeability for the three samples and three techniques in Figure 4.

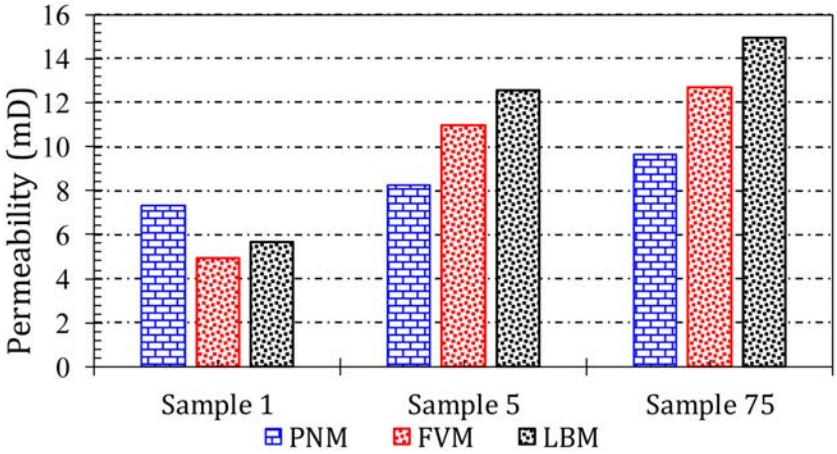

Figure 4—The results of the permeability prediction on the three samples.

While FVM and LBM are in good agreement, a discrepancy is observed for the PNM techniques in line with findings elsewhere (Dong & Blunt, 2009). The simulation time of the LBM is an order of magnitude longer than for the FVM, while the PNM runs instantly once the network is extracted, which is a relatively fast operation by using the modified maximal ball algorithm. Overall, the computation time between LBM (~2400 s) and PNM (~1 s) is more than three orders of magnitude in CPU time. The main benefit of the PNM is that the simplified geometry makes it possible to efficiently simulate much larger 3D digital rock volumes. While the PNM can suffer from a lack of accuracy, it can easily be used to provide an insight into the multiphase flow properties within porous media. Due to its simplicity, PNM is traditionally used to compute both single and multiphase petrophysical properties of rocks within the DRP framework. The strategy of taking advantage of deep learning for the permeability prediction was undertaken and is described below.

Application of Shallow and Deep Learning Techniques

Data Generation and Analysis for Machine Learning

A dataset consisting of 1,100 segmented images of 100x100x160 voxels was extracted from a complex carbonate rock and subsequently analyzed for ML purposes (Figure 1). Additionally, data of 400 samples from the literature were considered for further validation of our approach. Due to its computational efficiency, we used the PNM technique to extract the following features for our ML approach: porosity (PHI), permeability (KPNM), formation resistivity factor (FF), median throat length to radius ratio (TR), and average connection number (CN). In addition to the features derived by the PNM, direct simulations using LBM were performed to compute the permeabilities of all the 1,100 samples. ML should significantly reduce the computational time compared to direct simulations with comparable accuracy. Finally, in order to assess the models' predictive capability, we used the R2-score, or coefficient of determination, to measure the predictive capability of the different algorithms tested.

We provide below (Figure 5) an overview of the dataset by representing the cross-plot of relevant features as functions of the permeability—as computed by the more accurate LBM technique. The results highlight the fact that the PNM cannot be predictive of the actual permeability of the sample. While the PNM is widely used for simulating petrophysical properties, these results suggest that this simplified representation should be corrected in order to be used as a reliable tool for prediction.

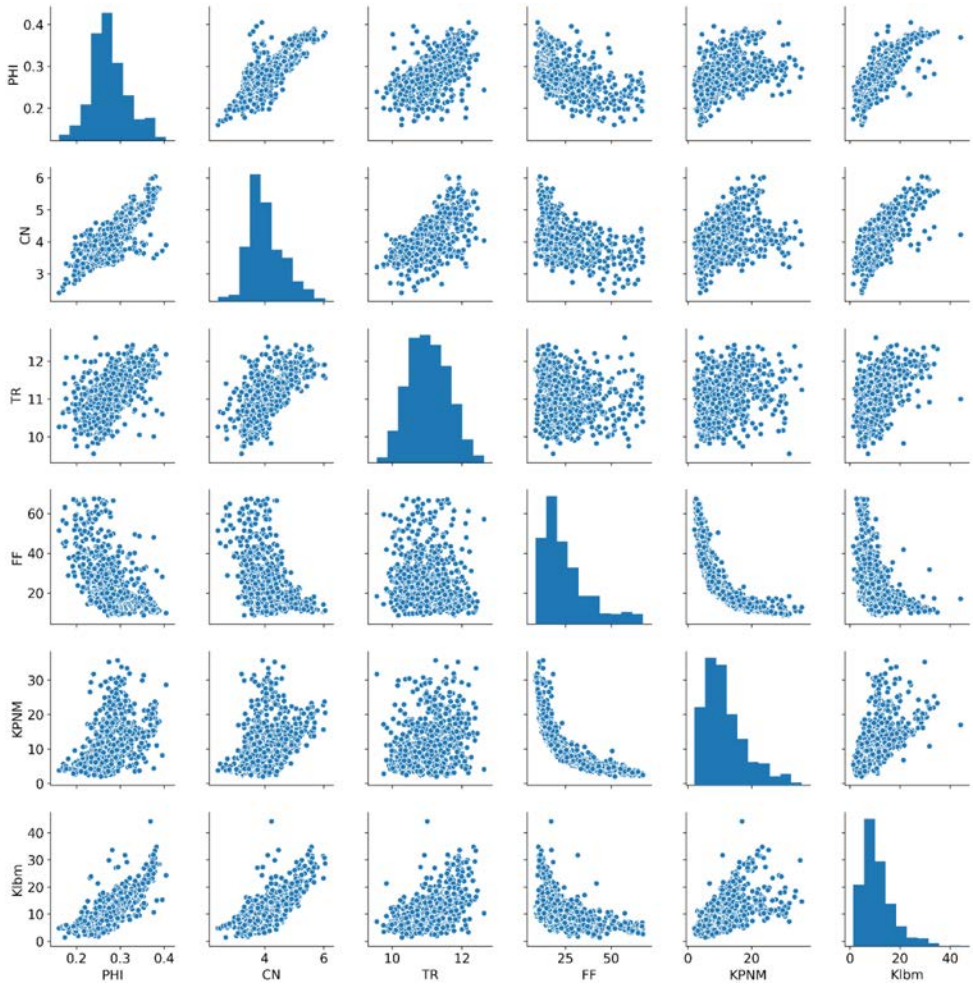

Figure 5—Statistics of the generated data for machine learning purposes.

Interestingly, if we focus on the cross-correlation between the PNM and the LBM methods (Figure 6), we observe that the predictive capability of the PNM is very limited for a complex carbonate, with a correlation coefficient R2-score of only 15.4%.

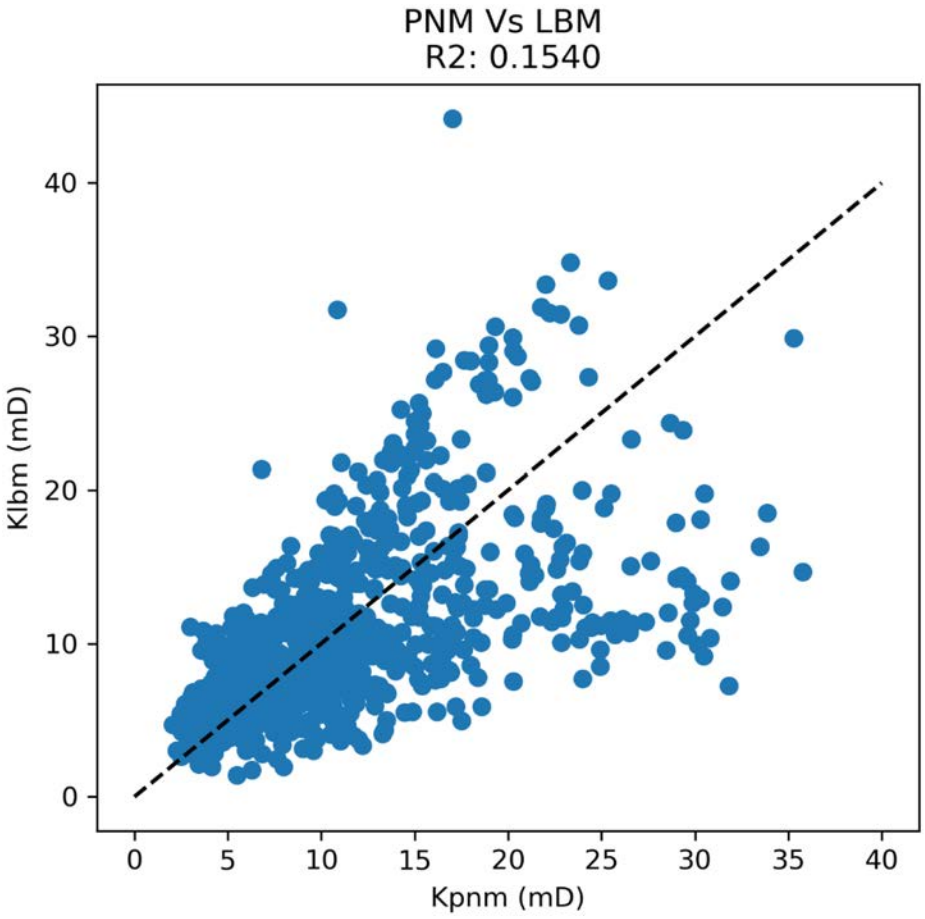

Figure 6—Cross-plot of the permeability predicted by the PNM and the LBM.

The goal in the present work was to improve the PNM's predictions of permeability by using machine and deep learning. We have used both supervised (i) shallow learning techniques and (ii) deep neural networks to infer the rock permeability. We first trained the model using the input (values of the selected features) and output (permeability values) of 70% the data previously generated, and subsequently used the model to predict the permeability of the remaining test dataset. Finally, with respect to the code implementation, it is worth noting that the regression supervised learning techniques were based on (*i*) shallow learning through the scikit-learn library and (*ii*) a deep learning algorithm using TensorFlow combined with Keras framework. All the codes used opensource libraries implemented in Python and C++.

Prediction

Supervised shallow learning. We used a regression problem aiming to predict a real-valued output. We used both linear and gradient boost techniques; in order to improve these two models, feature-cross (FC) techniques are investigated as well. Of the 1,100 samples, 70% of the dataset was used for training, while the remaining 30% was used for testing. After fitting the model on the training data, we obtained in Figure 7 the results of the predictions made by using linear regression (LR) and gradient boost (BG) algorithms on the test dataset. We can observe a slight improvement using gradient boost method compared to the linear regression model, with an R2-score of nearly 79.6%.

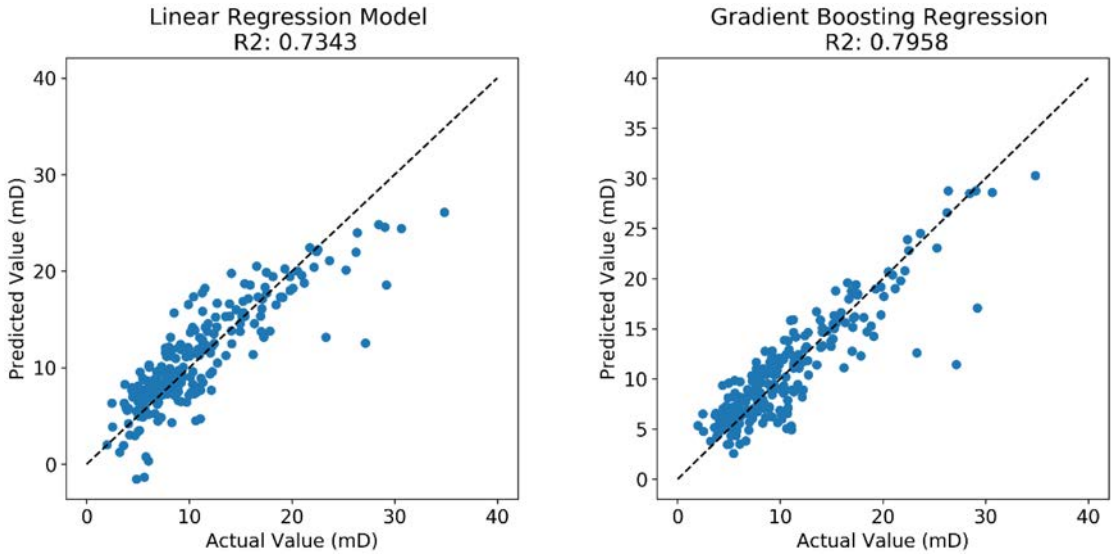

Figure 7—The prediction of permeability using (left) linear regression and (right) gradient boost regression algorithms, respectively.

It is worth noting that the hyperparameters used for the model were optimized using a technique combining grid search and k-fold cross-validation. In the case of gradient boost, this led to the hyperparameters for the learning rate and number of estimators presented in Figure 8. We chose a learning rate of 0.1 and an estimator of 100 for the gradient boost algorithm.

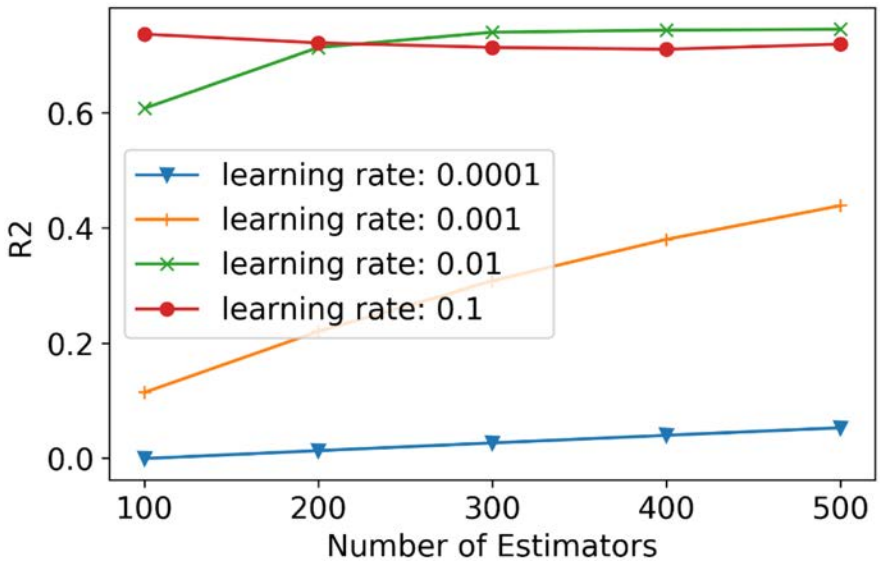

Figure 8—Hyperparameters optimization analysis

Finally, we used feature-cross techniques in order to boost the performance of the ML algorithm. The term feature-cross refers to a synthetic feature that encodes nonlinearity in the feature space by multiplying two or more input features together. We found that the best feature-cross corresponded to polynomial combinations of the features with degree less than or equal to 2 for the gradient boost algorithm (Figure 9), showing a better performance compared to the case in Figure 7 without feature-cross.

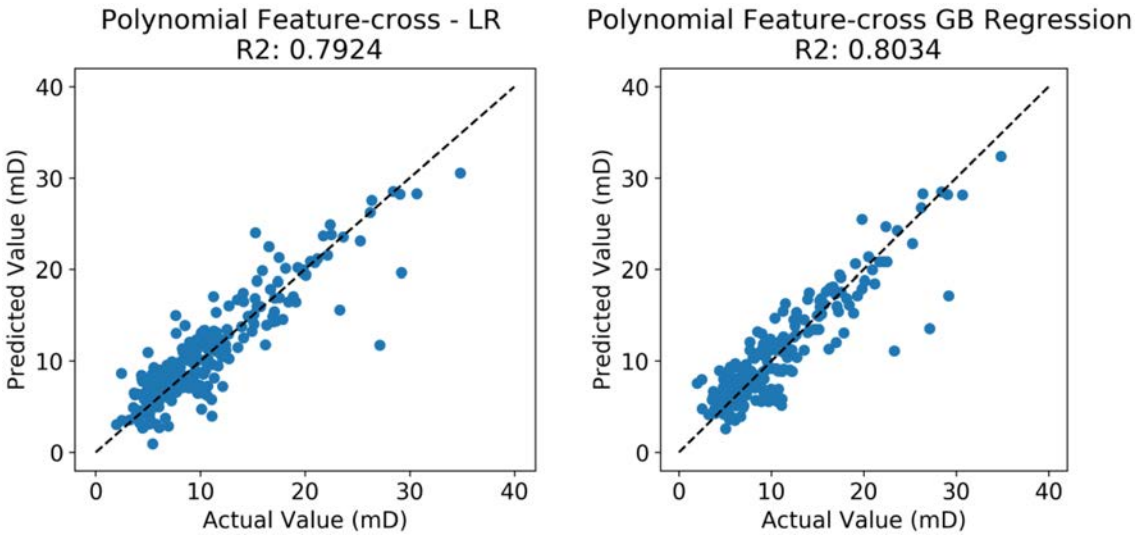

Figure 9—Feature-cross using polynomial combinations of the features with degree ≤ 2 for both (left) linear regression and (right) gradient boost algorithms.

Next, the performance was slightly improved to an R2-score above 81% by using the xboost gradient (XGB) and random forest (RF) algorithms (Figure 10).

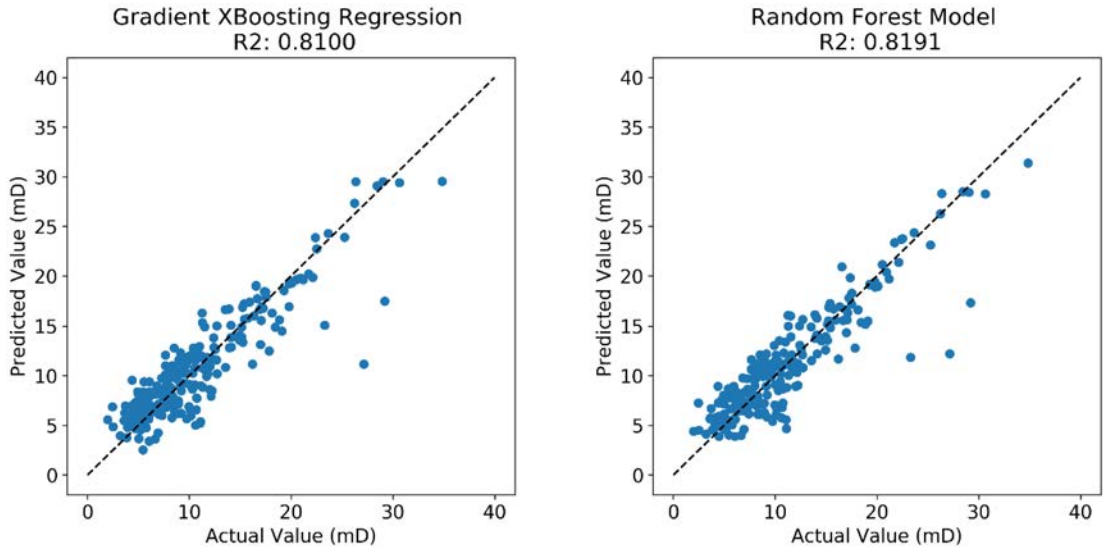

Figure 10—The prediction of permeability using (left) xboost gradient and (right) random forest regression algorithms, respectively.

Deep Learning from a Deep Neural Network. To complement the previous analysis in machine leaning, here we used deep learning based on multilayer perceptron architecture to investigate the permeability based on the features derived previously. In order to make the model non-linear, an activation function was used such that the relation between the input ($\boldsymbol{x}$) and output ($\boldsymbol{y}$) of one layer can be represented as:

$$y = \sigma[wx + b] \tag{6}$$

The rectified linear unit (ReLU) activation function, σ, is used in the present study. Eq. (6) illustrates a neural network of a single hidden layer mapping the feature vector $\boldsymbol{x}$ to the output vector $\boldsymbol{y}$ through the bias, b, and weight, w. A deep neural network (DNN) is defined as sequential layers that data flow through, consisting of connected nodes of multiple layers. The architecture of the densely-connected feed-forward network we tested consisted of 2 hidden layers of 10 nodes and is depicted in Figure 11.

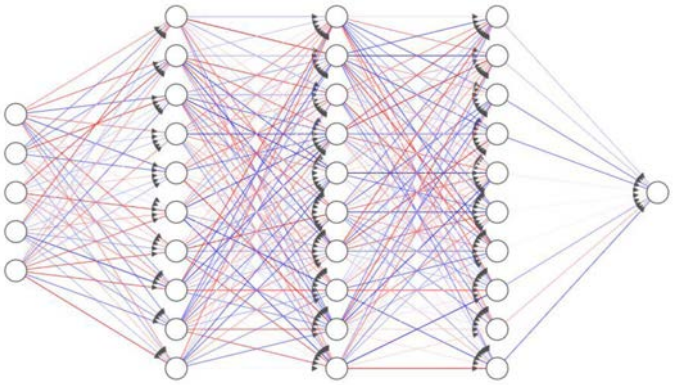

Figure 11—Architecture used for the deep neural network model.

The result of the prediction by the DNN is shown in Figure 12, which provides better performance compared to the previous ML algorithms. We can expect even better performance with a larger dataset.

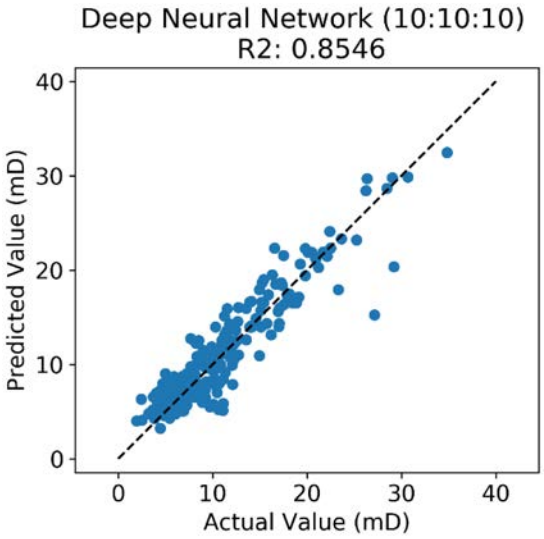

Figure 12—Prediction by DNN using the base model architecture.

Next, we tested the model on a new dataset from the literature consisting of 400 samples. The results for an optimized DNN are shown below in Figure 13, with R2-score at more than 91%. It is worth noting that the DNN model was optimized from the architecture in Figure 11 by using the Tensorboard toolkit integrated into TensorFlow.

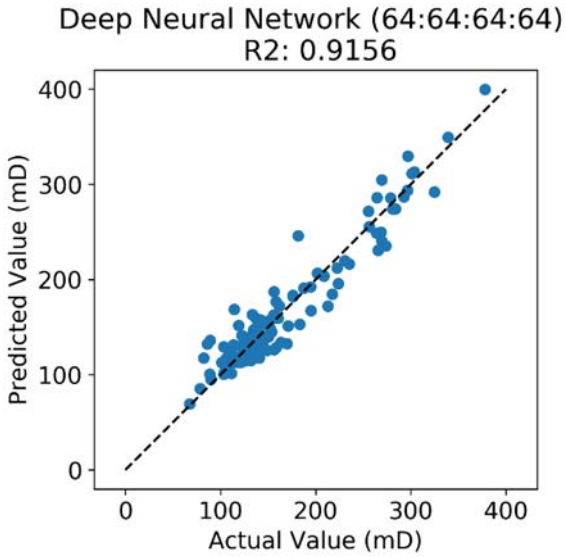

Figure 13—Prediction by DNN applied to the sandstone dataset.

Finally, we implemented a convolution neural network (CNN) approach. This model used only the raw segmented images alone and was not able to predict the permeability with an accuracy of more than 64%. The architecture of the CNN model is given below (Figure 14). The CNN consisted of two convolutional layers, one pooling layer, and three fully-connected layers. To improve the performance of the CNN model, we extended it to include some additional features, such as the porosity, and formation factor. Although this model is more complete, we did not observe an improvement in terms of performance. Again, the lack of a large set of data could explain the lack of improvement observed for deep learning based on the CNN model.

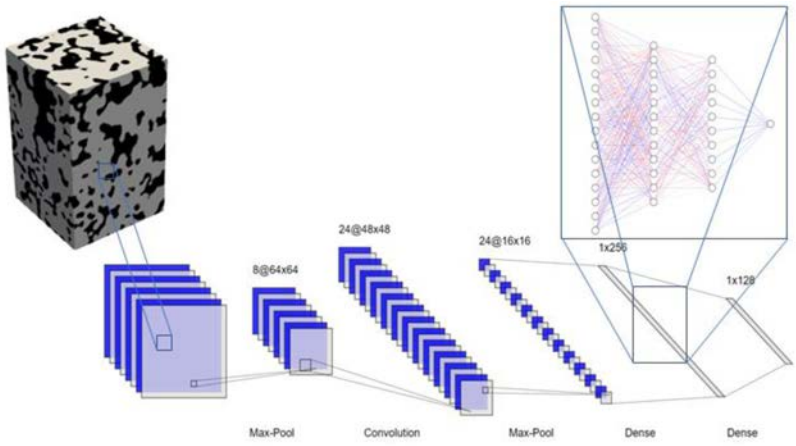

Figure 14—Schematic of the CNN network for the permeability prediction.

We show below in Figure 15 a summary of the R2-scores of the different algorithms used in the present study. Interestingly, all the algorithms performed better than the PNM computation of the permeability.

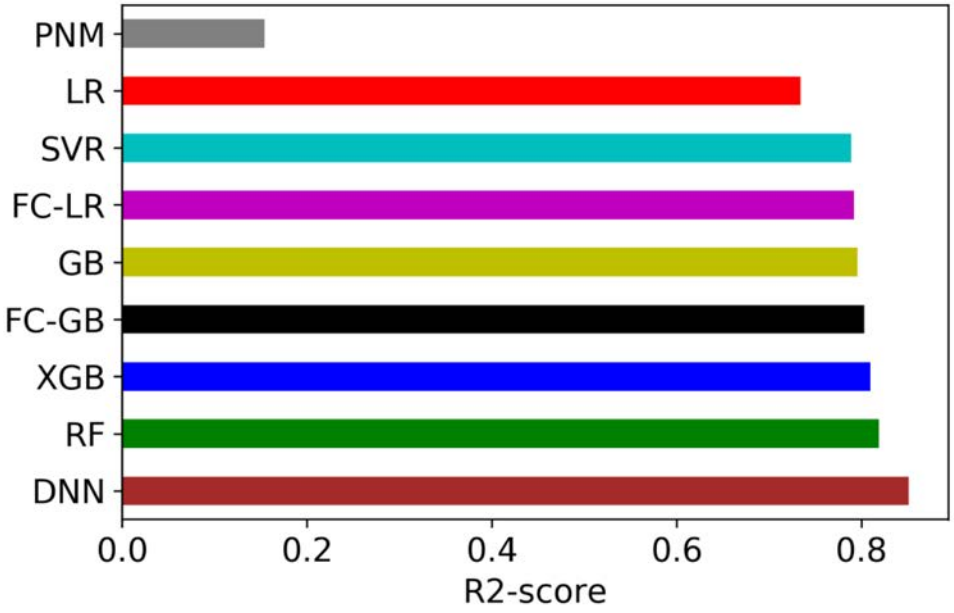

Figure 15—Summary of R2-score of the different machine and deep leaning algorithms used.

Finally, while the model has only been trained on a small subset of 3D images of 100x100x160 voxels, when we applied it to a larger sample of 500x500x920 voxels by extracting its features, the ML provided a permeability of 12.03 mD in less than a second compared to the value of 12.38 mD in a day by running the LBM simulation. This highlights the capability of ML to accurately estimate (within 3% of error) complex and heterogenous rock petrophysical properties.

Conclusion

We developed a workflow for fast and accurate prediction of the permeability of complex carbonate from the Middle-East. This data-driven approach is based on machine and deep learning in conjunction with numerical techniques, including the pore-network and lattice Boltzmann techniques. To take advantage of the efficient computation provided by PNM and the accuracy of the LBM, a wide range of ML algorithms has been investigated to infer the permeability of rock images scanned at high resolution. Different machine learning (deep or not) algorithms have been tested on a dataset containing more than a thousand micro-CT 3D images, from which relevant features, such as the porosity, the formation factor, and the 3D images, are extracted and fed into supervised shallow and deep learning models to compute the permeability. It is found that the deep neural network performs slightly better than gradient boosting and linear regression with feature crossing. The results provide a workflow for predicting the petrophysical properties of rock samples based on micro-CT images. With our data-driven workflow, simulations that could take days would only need a few seconds when a trained network is used. For perspective, the predictions made by convolution neural networks based solely on raw images could be improved to help limit the features engineering required to predict petrophysical properties.

Acknowledgements

The authors gratefully acknowledge Khalifa University supercomputing resources (HPCC) made available for conducting the research reported in this paper. The authors would also like to thank ADNOC for facilitating this research work.

References

Andrä, H., Combaret, N., Dvorkin, J., Glatt, E., Han, J., Kabel, M., … Zhan, X. (2013a). Digital rock physics benchmarks-Part I: Imaging and segmentation. *Computers and Geosciences*. https://doi.org/10.1016/j.cageo.2012.09.005

Andrä, H., Combaret, N., Dvorkin, J., Glatt, E., Han, J., Kabel, M., … Zhan, X. (2013b). Digital rock physics benchmarks-part II: Computing effective properties. *Computers and Geosciences*. https://doi.org/10.1016/j.cageo.2012.09.008

Blunt, M. J., Bijeljic, B., Dong, H., Gharbi, O., Iglauer, S., Mostaghimi, P., … Pentland, C. (2013). Pore-scale imaging and modelling. *Advances in Water Resources*, **51**, 197–216. https://doi.org/10.1016/j.advwatres.2012.03.003

Chung, T., Wang, Y. D., Armstrong, R. T., & Mostaghimi, P. (2019). Approximating Permeability of Microcomputed-Tomography Images Using Elliptic Flow Equations. https://doi.org/10.2118/191379-PA

Dehghan Khalili, A., Arns, J.-Y., Hussain, F., Cinar, Y., Pinczewski, W., & Arns, C. H. (2013). Permeability Upscaling for Carbonates From the Pore Scale by Use of Multiscale X-Ray-CT Images. *SPE Reservoir Evaluation & Engineering*, **16**(04), 353–368. https://doi.org/10.2118/152640-PA

Dong, H., & Blunt, M. J. (2009). Pore-network extraction from micro-computerized-tomography images. *Physical Review E - Statistical, Nonlinear, and Soft Matter Physics*, **80**(3), 1–11. https://doi.org/10.1103/PhysRevE.80.036307

Guibert, R., Nazarova, M., Horgue, P., Hamon, G., Creux, P., & Debenest, G. (2015). Computational Permeability Determination from Pore-Scale Imaging: Sample Size, Mesh and Method Sensitivities. *Transport in Porous Media*, **107**(3), 641–656. https://doi.org/10.1007/s11242-015-0458–0

Kegang, L. (2012). Correlation between Rock Permeability and Formation Resistivity Factor-A Rigorous and Theoretical Derivation. *Society of Petroleum Engineers Middle East Unconventional Gas Conference and Exhibition*, **10**. https://doi.org/10.2118/152724-MS

Kohli, A., & Arora, P. (2014). *IPTC 17475 Application of Artificial Neural Networks for Well Logs*. Retrieved from https://www.onepetro.org/download/conference-paper/IPTC-17475-MS?id=conference-paper%2FIPTC-17475-MS

Mostaghimi, P., Blunt, M. J., & Bijeljic, B. (2013). Computations of Absolute Permeability on Micro-CT Images. *Mathematical Geosciences*, **45**(1), 103–125. https://doi.org/10.1007/s11004-012-9431–4

Nwachukwu, A., Jeong, H., Pyrcz, M., & Lake, L. W. (2018). Fast evaluation of well placements in heterogeneous reservoir models using machine learning. *Journal of Petroleum Science and Engineering*, **163**, 463–475. https://doi.org/10.1016/J.PETROL.2018.01.019

Singh, N. P. (2019). Permeability prediction from wireline logging and core data: a case study from Assam-Arakan basin, **9**, 297–305. https://doi.org/10.1007/s13202-018-0459-y

Sudakov, O., Burnaev, E., & Koroteev, D. (2018). *Driving Digital Rock towards Machine Learning: predicting permeability with Gradient Boosting and Deep Neural Networks*. Retrieved from https://arxiv.org/pdf/1803.00758.pdf

Tembely, M., AlSumaiti, A. M., Jouini, M. S., & Rahimov, K. (2017). The effect of heat transfer and polymer concentration on non-Newtonian fluid from pore-scale simulation of rock X-ray micro-CT. *Polymers*, **9**(10). https://doi.org/10.3390/polym9100509

Wu, J., Yin, X., & Xiao, H. (2018). Seeing permeability from images: fast prediction with convolutional neural networks. *Science Bulletin*, **63**(18), 1215–1222. https://doi.org/10.1016/j.scib.2018.08.006

Xie, C., Raeini, A. Q., Wang, Y., Blunt, M. J., & Wang, M. (2016). An improved pore-network model including viscous coupling effects using direct simulation by the lattice Boltzmann method. *Advances in Water Resources*, **100**, 26–34. https://doi.org/10.1016/j.advwatres.2016.11.017

Yala, A., Lehman, C., Schuster, T., & Barzilay, R. (2019). A Deep Learning Mammography-based Model for Improved Breast Cancer Risk Prediction • Content code. *Radiology*, **292**, 60–66. https://doi.org/10.1148/radiol.2019182716